Solid-State Electronics Vol. 32, No. 12, pp. 1101–1108, 1989
Printed in Great Britain. All rights reserved

0038-1101/89 $3.00 + 0.00
Copyright © 1989 Pergamon Press plc

ELECTRICAL AND SPECTROSCOPIC STUDIES OF SPACE-CHARGE BUILDUP, ENERGY RELAXATION AND MAGNETICALLY ENHANCED BISTABILITY IN RESONANT-TUNNELING STRUCTURES

L. Eaves°, M. L. Leadbeater°, D. G. Hayes°*, E. S. Alves°, F. W. Sheard°, G. A. Toombs°, P. E. Simmonds°*, M. S. Skolnick*, M. Henini° and O. H. Hughes°

°Department of Physics, University of Nottingham, Nottingham NG7 2RD, England.
*RSRE, St. Andrews Road, Great Malvern, Worcestershire WR14 3PS, England.

ABSTRACT

Photoluminescence measurements and magnetoquantum oscillations in the differential capacitance are used to measure space-charge buildup and study electron thermalization in a double-barrier resonant tunneling structure based on n-type (AlGa)As. The intrinsic bistability observed in the I(V) characteristics is also seen in the linewidth and photon energy of the photoluminescence. The spectroscopic data reveal clearly the importance of intersubband transitions in the voltage range at which electrons tunnel resonantly into the second bound state of the quantum well. A novel field-induced enhancement of the intrinsic bistability effect is reported for $\underline{B} \| \underline{J}$.

INTRODUCTION

Two major themes of this and the previous HCIS conference have been the remarkable electrical properties of resonant tunneling and superlattice devices and the use of optical techniques to probe the energy distribution of carriers in quantum wells. Although resonant tunneling in a double-barrier semiconductor heterostructure was demonstrated fifteen years ago (Chang, Esaki and Tsu, 1974), the field is still extremely active. As a result of the improvement of material quality, resonant tunneling and novel magneto-electric quantization effects have been observed in devices with well widths up to 180 nm (Alves and co-workers, 1989; Eaves and co-workers, 1988; England and co-workers, 1989; Henini and co-workers, 1989). Considerable interest and controversy has been generated by the argument about whether resonant tunneling should be regarded as a coherent or sequential process (Payne, 1986; Weil and Vinter, 1987; Luryi, 1985). In the sequential model, resonantly tunneling electrons undergo scattering processes in the quantum well, thereby losing quantum mechanical phase coherence before tunneling out through the collector barrier. When the second barrier has a relatively low transmission coefficient, a significant electronic space-charge can build up in the well at resonance (Ricco and Azbel, 1984). This charge must be taken into account when considering the current-voltage characteristics, I(V), (Goldman and co-workers, 1987a,b; Payling and co-workers, 1988; Sheard and Toombs, 1988). Recently, Young and co-workers (1988) demonstrated the potential of photoluminescence spectroscopy as a means of probing the electrons in the quantum well under resonant tunneling conditions.

This paper describes how a combination of magnetotransport, capacitance-voltage and photoluminescence measurement can provide detailed information about space-charge and energy relaxation effects in resonant tunneling devices. In structures with barriers of different thicknesses (Alves and co-workers, 1988; Leadbeater and co-workers, 1988), or different heights (Zaslavsky and co-workers, 1988) a large buildup of charge in the well is expected at resonance when electrons are injected through the thinner emitter barrier and are inhibited from tunneling out due to the lower transmission coefficient of the thicker collector barrier. This leads to intrinsic bistability in I(V). The magneto-oscillations in the differential capacitance and tunnel current monitor both the space-charge buildup in the quantum well and in the accumulation layer of the emitter contact. In contrast to previous studies of magnetoquantum oscillations in symmetric DBS's (Goldman, Tsu and Cunningham, 1987b; Payling and co-workers, 1987) we find that the quasi-Fermi level of the electrons stored in the well lies significantly below the Fermi level of the electrons in the emitter accumulation layer. We attribute this to energy relaxation of the stored charge distribution which will occur if the electron storage time in the quantum well is sufficiently long. Estimates of this storage time obtained experimentally and theoretically are consistent with this hypothesis. The resonant tunneling process in our asymmetric DBS is thus truly sequential rather than coherent. We also demonstrate how a magnetic field, applied perpendicular to the plane of the tunnel barriers ($B \| J$) can lead to a strong enhancement of intrinsic bistability as a result of the large degeneracy of Landau states in the quantum limit (Leadbeater and Eaves, 1989).

DETAILS OF STRUCTURE OF THE DEVICE

Our asymmetric structure consisted of the following layers in order of growth from the n^+GaAs substrate: (i) 2 μm GaAs, doped to 2 x 10^{18} cm^{-3}, (ii) 50 nm GaAs, 10^{17} cm^{-3}, (iii) 50 nm GaAs, 10^{16} cm^{-3}, (iv) 3.3 nm GaAs, undoped, (v) 8.3 nm $Al_{0.4}Ga_{0.6}As$, undoped (thin barrier), (vi) 5.8 nm GaAs, undoped (well), (vii) 11.1 nm $Al_{0.4}Ga_{0.6}As$, undoped (thick barrier), (viii) 3.3 nm GaAs, undoped, (ix) 50 nm GaAs, 10^{16} cm^{-3}, (x) 50 nm GaAs, 10^{17} cm^{-3} (xi) 0.5 μm GaAs, 2 x 10^{18} cm^{-3}, top contact. The layers were processed into mesas of diameter 200 μm. The conduction-band profile with the top contact biased positively, is shown in Fig. 1. A bound state is formed in the accumulation region adjacent to the emitter barrier and, at liquid helium temperatures, the associated two-dimensional electron gas (2DEG) is degenerate. The accumulation potential may be modelled satisfactorily using a variational solution for the bound-state wave function. At a bias of 330 mV the electric field in the emitter barrier is 29 kV cm^{-1} and the width of the accumulation region is ~14 nm. In the remainder of this layer (~36 nm) the Fermi level is close to the conduction-band edge since the doping density (10^{16} cm^{-3}) is close to the Mott metal-insulator transition. However, this does not give rise to an important series resistance as shown by previous studies of similarly doped single-barrier structures.

MAGNETOTUNNELING AND CAPACITANCE MEASUREMENTS

The current-voltage characteristic for our asymmetric DBS at 4 K is shown in Fig. 2 for the region corresponding to resonant tunneling into the first quasi-bound state of the quantum well. The region of the second resonance is considered later. The figure shows clearly the threshold for resonant tunneling at V_{th} = 330 mV, the turn-off at V_p = 725 mV where the current peaks, and the region of intrinsic bistability. The transverse components of momentum and hence transverse kinetic energy are conserved in the resonant tunneling process. Total energy is also conserved so resonant tunneling occurs when the energies of the bound states in the accumulation layer and quantum well essentially coincide. However, because of finite level widths, the tunneling rate from emitter into well will be a sharply peaked resonant function of the voltage drop across the emitter barrier. The observed resonant tunneling range V_{th} to V_p corresponds to climbing up this resonance peak. It is the screening effect of the charge buildup in the quantum well (electrostatic feedback) that is responsible for the extended voltage range over which resonant tunneling is observed in the I(V) curve and the appearance of current bistability. When the applied voltage is increased, only a very small voltage change across the emitter barrier is needed to charge up the well and, due to the screening effect of this charge, almost all the extra voltage drop occurs across the collector barrier and depletion layer. When biased in the opposite direction a very sharp maximum in the I(V) curve is observed (Alves and co-workers, 1988) since in this case (thin collector barrier) there is little charge buildup and electrostatic feedback is negligible. The bistability does not then appear.

Conservation of transverse kinetic energy in resonant tunneling requires the Fermi levels in the accumulation layer and quantum well to coincide. But the theory of resonant tunneling (Sheard and Toombs, 1988) shows that the states of transverse motion in the well are only partially occupied, since the occupancy is determined dynamically by the balance between the transition rates into and out of the well. However, if the energy relaxation time is much less than the charge storage time in the well, the electron distribution will be able to thermalize to the lattice temperature and establish a well-defined quasi-Fermi level below that in the emitter contact. This is the situation illustrated in Fig. 1. The Fermi energy of a thermalized 2DEG in the quantum well is less than the Fermi energy of the 2DEG in the accumulation layer since the bound-state levels essentially coincide during resonant tunneling.

We have investigated this possibility by studying magneto-oscillations in the capacitance of the structure for a magnetic field $\underline{B} \| \underline{J}$. In this geometry the states of transverse motion of a degenerate 2DEG (in emitter or well) are quantized into Landau levels. Theoretically, oscillations with a definite period $\Delta(1/B)$ in 1/B arise from a modulation of the charge when Landau levels pass through the quasi-Fermi level. This charge modulation affects the distribution of electric potential and screening lengths and hence modulates the capacitance of the device. The frequency of the oscillations $B_f = \{\Delta(1/B)\}^{-1}$ is thus related to the Fermi energy E_F by $B_f = m^*E_F/eh$, where m^* is the effective mass. For fully, as opposed to partially, occupied states $E_F = h^2\pi n/m^*$, where n is the areal electron density. This gives $n = 2eB_f/h$.

The voltage dependence of the differential capacitance C and parallel conductance G = 1/R are also plotted in Fig. 2. The differential parameters were measured at 1 MHz with a modulation of 3 mV using a Hewlett-Packard 4275A LCR meter in the mode which analyses the impedance of a device as a capacitor C and parallel resistor R. Between 10 kHz and 2 MHz these parameters are also independent of measurement frequency. Fig. 3 shows typical oscillatory structure in the variation of capacitance with magnetic field. Similar oscillations are also observed in the current I and conductance G but are less well defined. To reveal more clearly multi-periodic behaviour we have Fourier analysed the experimental capacitance traces. The distributions of magneto-oscillation frequencies B_f thus obtained are shown in Fig. 4 for different applied voltages.

Below the threshold voltage V_{th}, there is a single peak in the magneto-oscillation spectrum. This peak is clearly associated with the 2DEG in the emitter accumulation layer, since the corresponding areal density n_a increases steadily with voltage up to V_{th} as shown in Fig. 5. Moreover, the static capacitance values, given by the ratio of total accumulation charge to applied voltage, are in good agreement with the ac values shown in Fig. 2 and are consistent

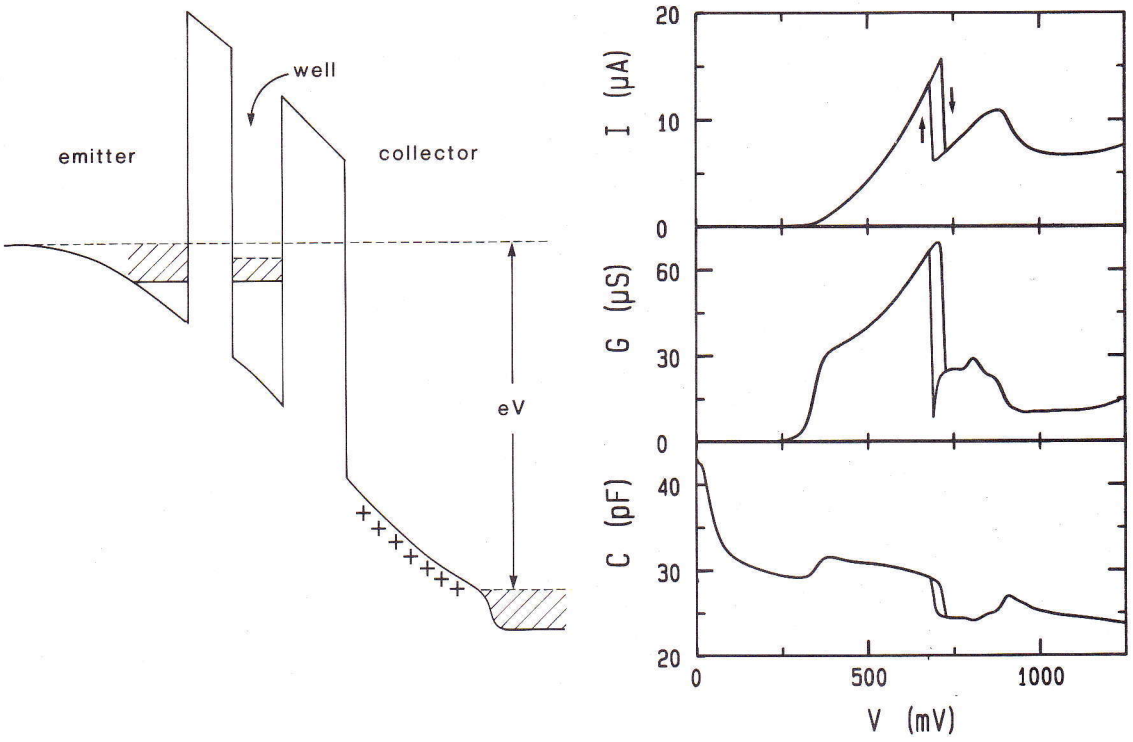

Fig. 1 *(left)* Conduction-band profile under applied voltage V showing bound-state levels (solid lines) in emitter and well and quasi-Fermi levels (dashed lines).

Fig. 2 *(right)* Voltage dependence of dc current I, ac capacitance C and parallel conductance G measured at 1 MHz and 4 K.

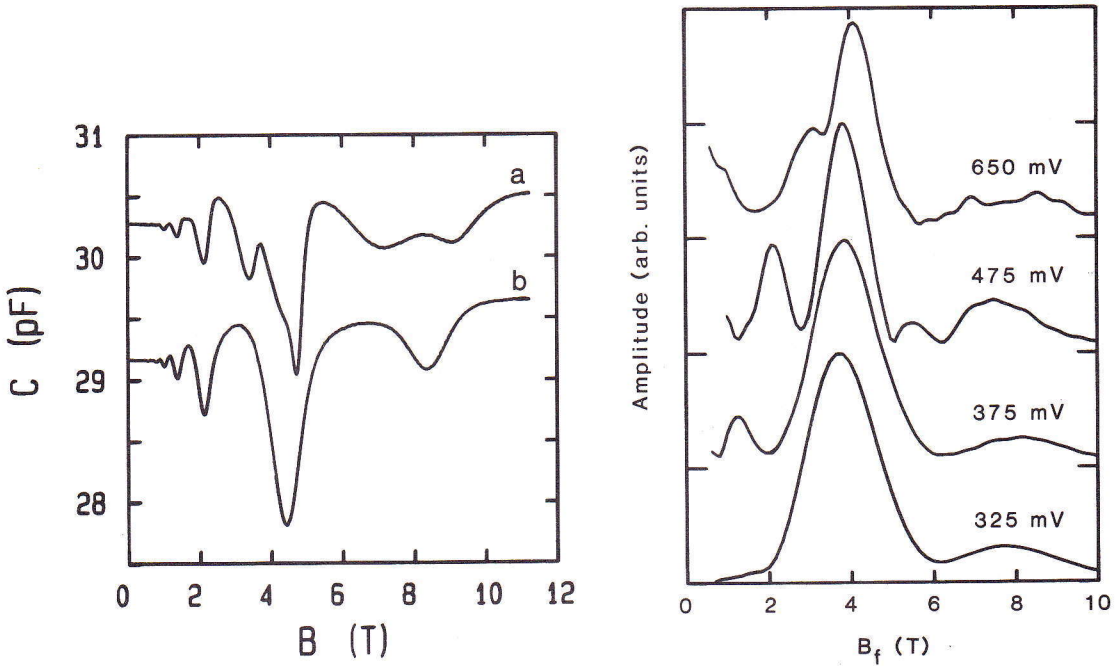

Fig. 3 *(left)* Magneto-oscillations in differential capacitance C vs. magnetic field B for applied voltage (a) 600 mV and (b) 300 mV.

Fig. 4 *(right)* Spectrum of the magneto-oscillation frequencies B_f obtained by Fourier transforming them in 1/B space. The peak position B_f for each voltage gives the inverse period. The weak structure at around 8 T corresponds to the second harmonic of the series due to the charge in the accumulation layer.

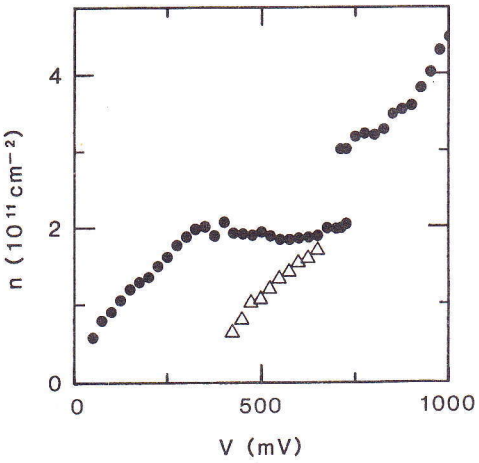

Fig. 5 Areal density n versus voltage V for charge in the accumulation layer n_a (circles) and well n_w (triangles). The values of n are deduced from the peaks in the Fourier spectrum.

with our theoretical modelling of the potential distribution across the heterostructure. We have also investigated the magneto-oscillations when the magnetic field is tilted at an angle θ to the normal to the layers. Up to $\theta = 40°$ the form of the oscillations as a function of $B\cos\theta$ is largely unchanged. This confirms the two-dimensional nature of the electrons in the emitter accumulation layer.

Between V_{th} and V_p, this magneto-oscillation frequency is independent of voltage (Fig. 4) and within experimental error, the accumulation density n_a remains constant at 2.2×10^{11} cm^{-2}. Hence the electric field and voltage drop across the emitter barrier remain virtually unchanged in this range, which is consistent with our model of resonant tunneling between bound states in the emitter and quantum well. Also in the resonant tunneling region, a second, weaker peak appears in the magneto-oscillation spectrum (Fig. 4). The frequency of this peak gives an areal density n_w, which increases throughout this range and approaches n_a at the voltage V_p for maximum current (Fig. 5). We attribute this peak to a degenerate electron distribution stored in the quantum well whose temperature $T_e \ll \hbar\omega_c/k = 15$ K at B = 1 T. The equality of n_a and n_w at $V = V_p$ is to be expected theoretically since the peak transition rate into the well is much greater than the decay rate out of the well throughout the collector barrier. The dynamically determined occupancy of the states in the well is then close to unity and energy relaxation has little effect on the electron distribution.

This cooling of the electrons is confirmed by comparing the lifetime τ_c of the electrons in the well with the energy relaxation rate. The lifetime τ_c is limited by tunneling through the collector barrier and is related to the current density by $J = n_w e/\tau_c$ (Sheard and Toombs, 1988). At the resonance peak ($J \simeq 0.06$ A cm^{-2}, $n_w \simeq 2 \times 10^{11}$ cm^{-2}) this gives $\tau_c \sim 0.6$ μs. The energy relaxation must be via spontaneous emission of acoustic phonons since the temperature is low (4 K) and the electron kinetic energies ($E_F \sim 7$ meV) are too small for optic-phonon processes. An estimate of the emission rate τ^{-1} from the deformation potential gives $\tau_{ph} \sim 10^{-9}$ s for a well-width of 5.8 nm. This is indeed much shorter than τ_c. We note that electron-electron scattering is not important here since the phonon emission rate is sufficiently large to thermalize the electron distribution to the lattice temperature within the available time τ_c.

When V increases above V_p a transition occurs in which charge is expelled from the well with a consequent redistribution of potential and resonant tunneling can no longer occur. This results in a step-wise increase in the accumulation layer density to $n_a \simeq 3 \times 10^{11}$ cm^{-2}, as shown in Fig. 5. For $V > V_p$ only a single magneto-oscillation period is observed. The different charge states of the device on the high- and low-current parts of the hysteresis loop are also clearly shown by the different magneto-oscillation frequencies observed. The corresponding sheet density increases smoothly with voltage showing that, in this case, there is little charge buildup in the well. We note here that the broad maximum in I(V) above the current bistability is due to inelastic tunneling processes which have been previously observed and discussed elsewhere (Leadbeater and co-workers, 1989).

The principal features of the C(V) curve of Fig. 2 can also be understood in terms of our model. We may regard the DBS as two parallel plate capacitors C_1 (emitter barrier and accumulation layer) and C_2 (collector barrier and depletion layer) connected in series. The charge on the common central plate corresponds to the charge stored in the quantum well. The steep fall in capacitance at low voltages is due to the rapid increase in depletion length in the lightly-doped (10^{16} cm^{-3}) collector layer which decreases C_2. The slower decrease for $V > 50$ mV is due to the less rapid rate of depletion of the layer doped to 10^{17} cm^{-3}. However, the most notable features are the sharp increase in capacitance at V_{th} and subsequent fall at V_p. When the bound states of the accumulation layer and quantum well are on resonance, the voltage drop across C_1 is essentially constant. An increase in applied voltage therefore appears almost entirely

across C_2. The measured differential capacitance is thus $C \simeq C_2$ in the resonant tunneling region, whereas off-resonance $C = C_1C_2/(C_1 + C_2) < C_2$.

This quasi-static argument is not obviously applicable at 1 MHz, where the measurements of differential capacitance were made. In a small-signal analysis (Sheard and Toombs, 1989) based on the sequential theory of resonant tunneling, C_1 and C_2 have parallel resistors R_1 and R_2 respectively. R_1 allows electrons tunneling from the emitter to charge the quantum well whilst R_2 allows the stored charge to leak through the collector barrier. Our previous argument is equivalent to the assumption that during resonant tunneling, R_1 becomes very small and effectively short-circuits C_1 so that the measured capacitance $C \simeq C_2$. By identifying the time constant R_2C_2 with the storage time τ_c we have $\tau_c = R_2C_2 \sim RC$ during resonance. The values shown in Fig. 2 give $\tau_c \sim 0.4$ μs at V_p, which is consistent with our previous estimate from the dc current and charge. An approximate theoretical estimate of τ_c can be made by calculating the attempt rate (obtained from the energy of the bound state above the bottom of the well ~ 68 meV) and the transmission coefficient of a rectangular barrier (conduction band offset ~ 320 meV). This gives $\tau_c \sim 1$ μs. Under bias a smaller value is expected since the average collector-barrier height is then decreased. Measurements of the tunneling escape time from the quantum well of a DBS have also been made by studying the temporal decay of photoluminescence (Tsuchiya and co-workers, 1987). However, the optical determination of τ_c is limited to thin-barrier structures for which τ_c is less than the radiative recombination time $\tau_r \sim 0.5$ ns. In our asymmetric structure it is the thick collector barrier which gives rise to the long τ_c.

PHOTOLUMINESCENCE MEASUREMENTS

The above picture of the resonant tunneling process is complemented by low temperature photoluminescence (PL) measurements (Hayes and co-workers, 1989). These were performed at 2 K using 1.96 eV incident radiation of low power density (< 1 W cm^{-2}) with the device in forward bias. Fig. 6 compares the I(V) characteristics, taken this time under weak illumination, with the key features of the PL data: PL intensity, linewidth and photon energy at the PL peak. The peak in I(V) at 2.4 V, not shown in Fig. 2, corresponds to resonant tunneling into the second quasibound state of the quantum well. This also shows a region of intrinsic bistability (Alves and co-workers, 1988). Detailed modelling of the device shows that on the second peak in I(V), the electronic space-charge is mainly in the lower state of the electron quantum well whereas the current mainly arises from electrons directly tunneling out of the upper state (see also Foster and co-workers, 1989).

The PL arises from electron-hole recombination between the lowest electron and heavy hole states in the quantum well. On resonance, the electrons present in the well arise predominantly from the charge buildup which occurs during the tunneling, whereas the holes are photocreated principally in the GaAs contact regions. The holes then diffuse and drift to the collector barrier where they accumulate and tunnel into the well (inset to Fig. 6).

Figure 6(a) shows the variation of PL peak energy with V. The PL peak energy corresponds to recombination of holes with electrons in the lower bound state of the (electron) quantum well, even when the device is biased for resonant tunneling of electrons into the second bound state. This indicates the importance of intersubband scattering in relaxing the energy of resonantly tunneling electrons. A large shift to lower energy of 20 meV at 3.3 V, due to the Stark shift of the electron and hole quasibound states, is observed. The shift is close to that expected for a ~60 Å well in an electric field of ~2 x 10^5 V cm^{-1}. There are two discontinuities and bistable regions in the variation of peak energy with bias (expanded version, Fig. 7), corresponding to those in I(V). These arise from the changes in the energies of the quasibound states in the well, and of the band gap renormalization, between the on- and off-resonant states.

The variation of PL linewidth versus bias is shown in Fig. 6(b), and on an expanded scale in Fig. 7. As V is swept, the linewidth increases up to the switch-off of the first resonance (0.7 V) where it falls sharply and remains fairly constant until the threshold voltage for the second resonance at ~1.7 V. Here the linewidth steadily increases with tunneling current up to the switch-off, where it again falls sharply and then stays constant in a similar manner to the first resonance. The variation of the linewidth with bias is very similar to that of the current, see Fig. 6(a). Bistability and accompanying hysteresis loops are again observed. The increase in PL linewidth with resonant current is due to free carrier broadening and indicates filling of electron states in the well, as confirmed by magnetic field measurements (Hayes and co-workers, 1989).

The change in linewidth between the on- and off- resonant states can be used to determine n_w at the resonances. For the first resonance, by convolving the lineshape observed off resonance (where $n_w \approx 0$) with a Fermi function (including a decreasing oscillator strength towards E_F), a good fit to the experimental spectrum can be obtained, and values of $E_F = 7.5 \pm 1.0$ meV and $n_w = (2.2 \pm 0.3) \times 10^{11}$ cm^{-2} deduced. This is in excellent agreement with that given by the electrical measurements (see Fig. 5). For the second resonance, the fitting is less reliable due to the absence of a sharp Fermi cut-off in the spectrum, but values of $E_F = 12 \pm 2$ meV and $n_w = (3.5 \pm 0.5) \times 10^{11}$ cm^{-2} are estimated. More accurate values for n_w, without any fitting procedure, are obtained from the magneto-PL measurements (Hayes and co-workers, 1989).

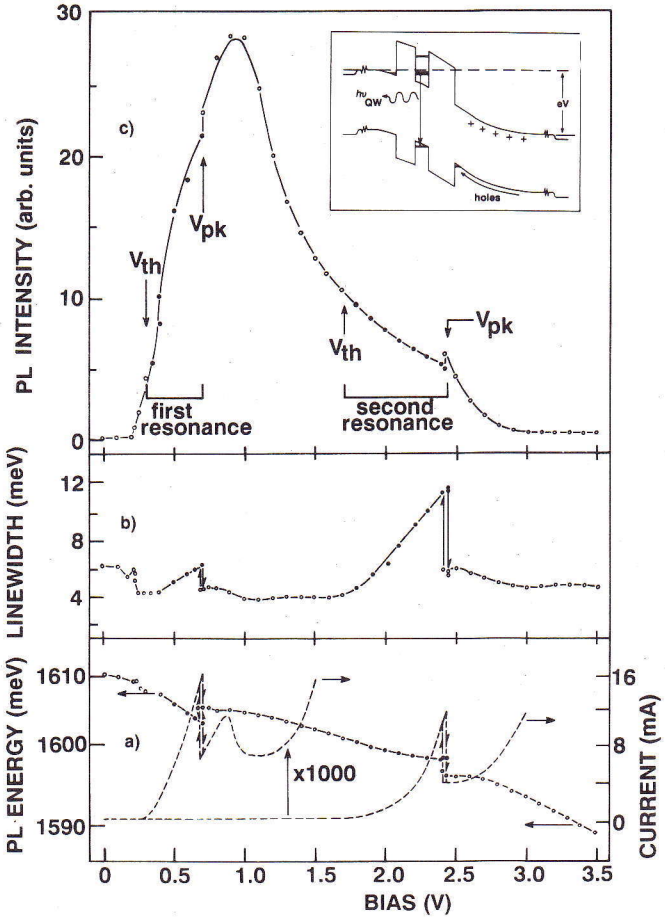

Fig. 6 Variation with bias voltage of current (Fig. 6(a) dashed); PL peak position (Fig. 6(a); circles), PL linewidth (full width half maximum) (Fig. 6(b)); integrated PL intensity (Fig. 6(c)). o - low I state, • - high I state. The bistable, hysteresis loops are exhibited in the bias dependence of the current, PL peak energy and linewidth. The inset shows a diagram of the energy bands and quasi-Fermi levels in the structure at the bias voltage of the first resonance.

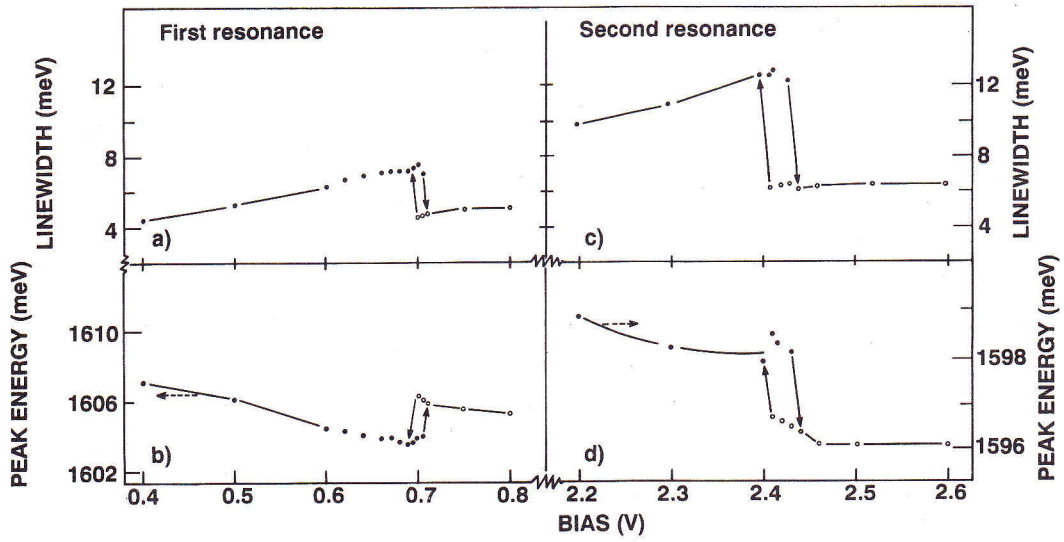

Fig. 7 Expanded plots of the variation of the PL peak energy and linewidth around the bistable regions of the first and second resonances.

Figure 6(c) shows the PL intensity as a function of V. The maximum of PL intensity occurs between the two resonances at 1.0 V where there is no electron charge buildup. In contrast to the model of Young and co-workers (1988) we therefore deduce that the PL intensity is not, in general, simply proportional to n_w in the quantum well, but also depends strongly on the population of the minority carrier holes in the well. Most of the holes which participate in the PL tunnel into the well through the thicker collector barrier. The effective height of the collector barrier to the holes is reduced with increasing bias, thus accounting in part for the rise in PL intensity between 0 and 1 V. The strong decrease of the PL signal from 1 to 3.3 V can be understood by reference to the inset of Fig. 6. When the bias is increase beyond 1 V, the injected holes will tunnel through the first barrier more easily, but with an increasing number passing straight over the second barrier. The dynamic hole population in the well will then fall with a consequent decrease in PL intensity as the bias is increased further (1.0 V to 3.5 V), in agreement with experiment.

MAGNETICALLY-INDUCED ENHANCEMENT OF INTRINSIC BISTABILITY

In the course of our magnetic field studies of asymmetric structures (Leadbeater and Eaves, 1989), we found that the voltage width of the intrinsic bistability on the first resonace peak in I(V) could be enhanced by the application of a magnetic field B applied perpendicular to the plane of the barriers (B‖J). This is illustrated in Fig. 8, which compares the zero field I(V) plot with those for 7 and 11.4 T and shows the principal bistability extending over a wider voltage range. Additional, weaker regions of bistability arise on the low current section of the principal bistability loop. In a quantizing magnetic field, the high current section of the principal bistability, labelled f → g on the 11.4 T plot, corresponds to resonant tunneling from the lowest (n = 0) Landau level of the 2DEG in the accumulation layer of the emitter to the n = 0 Landau level of the lower quasibound state of the quantum well. The bistability at B = 0 is controlled by the amount of negative space-charge that resides in the quantum well at resonance.

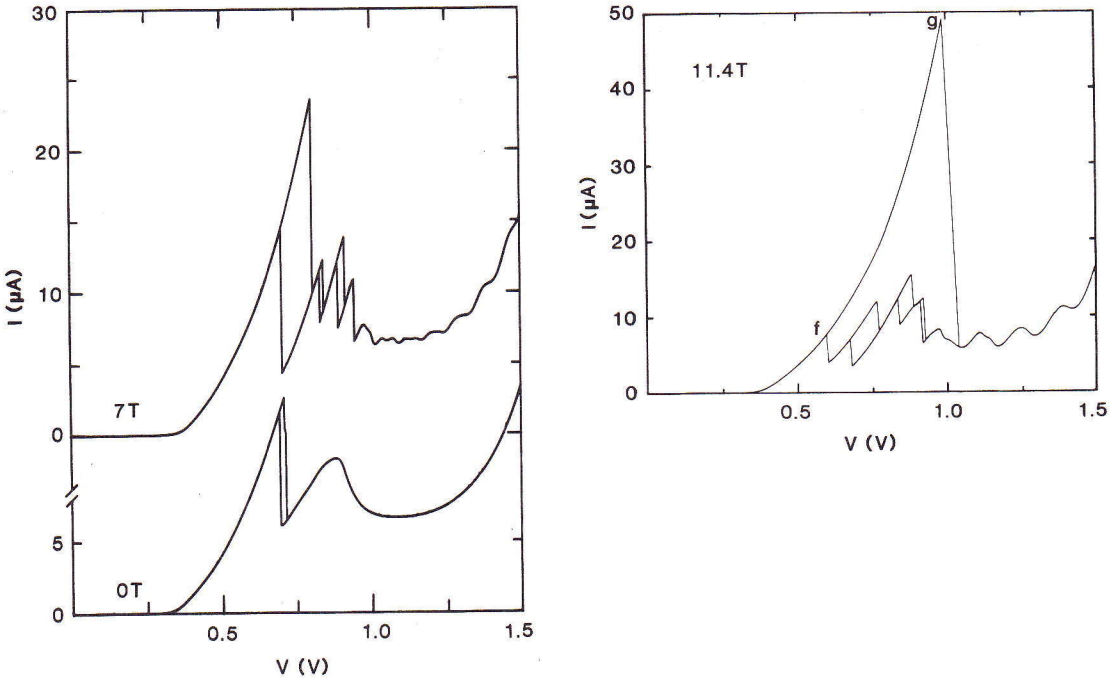

Fig. 8 I(V) plots at T = 4 K for B = 0, 7 and 11.4 T (B‖J) showing the magnetic field enhancement of the intrinsic bistability on the first resonance in forward bias.

This is a maximum (~2.2 x 10^{11} cm^{-2}) when the quasi-Fermi levels in the emitter 2DEG and quantum well are equal. In a magnetic field, the degeneracy (including spin) of each Landau level is 2eB/h. Therefore, the lowest Landau level of the lower bound state of the well can hold an electron density which increases linearly with B and can greatly exceed the value at B = 0. The voltage at the current peak of the bistability increases with B at a rate which is consistent with an electron sheet density in the well of 2eB/h. The additional, smaller regions of bistability on the 7 and 11.4 T plots are due to space-charge buildup arising from transitions involving a change in Landau level index from accumulation layer to quantum well. This can occur by elastic scattering or by the emission of a longitudinal optic phonon (Leadbeater and co-workers, 1989).

CONCLUSION

We have described the use of high magnetic fields and photoluminescence techniques to reveal new phenomena in resonant tunneling structures. Particular emphasis has been placed on the importance of space-charge buildup, its role in intrinsic bistability and energy relaxation effects.

ACKNOWLEDGEMENTS

This work is supported by SERC (U.K.). One of us (ESA) is supported by CNPq, Brazil. P. E. Simmonds is on leave from the University of Wollongong, NSW, Australia.

REFERENCES

Alves, E. S., L. Eaves, M. Henini, O. H. Hughes, M. L. Leadbeater, F. W. Sheard, G. A. Toombs, G. Hill and M. A. Pate (1988). *Electronics Lett.* 24, 1190. In this paper the bias direction for occurrence of intrinsic bistability was referred to as "reverse bias".

Alves, E. S., M. L. Leadbeater, L. Eaves, M. Henini, O. H. Hughes, A. Celeste, J. C. Portal, G. Hill and M. A. Pate (1989). *Superlattices and Microstructures* 4, 527.

Chang, L. L., L. Esaki and R. Tsu (1974). *Appl. Phys. Lett.* 24, 593.

Eaves, L., E. S. Alves, T. J. Foster, M. Henini, O. H. Hughes, M. L. Leadbeater, F. W. Sheard, G. A. Toombs, K. Chan, A. Celeste, J. C. Portal, G. Hill and M. A. Pate (1988). *Physics and Technology of Submicron Structures*, Springer Series in Solid-State Sciences 83, 74. Eds. H. Heinrich, G. Bauer, F. Kuchar.

England, P., J. R. Hayes, M. Helm, J. P. Harbison, L. T. Florez and S. J. Allen, Jr. (1989). *Appl. Phys. Lett.* 54, 1469.

Fang, F. F. and W. E. Howard (1966). *Phys. Rev. Lett.* 16, 797.

Foster, T. J., M. L. Leadbeater, D. K. Maude, E. S. Alves, L. Eaves, M. Henini, O. H. Hughes, A. Celeste, J. C. Portal, D. Lancefield and A. R. Adams (1989). *These Proceedings.*

Goldman, V. J., D. C. Tsui and J. E. Cunningham (1987a). *Phys. Rev. Lett.* 58, 1257.

Goldman, V. J., D. C. Tsui and J. E. Cunningham (1987b). *Phys. Rev. B* 35, 9387.

Hayes, D. G., M. S. Skolnick, P. E. Simmonds, L. Eaves, D. P. Halliday, M. L. Leadbeater, M. Henini and O. H. Hughes (1989). *Proc. 4th Int. Conf. on Modulated Semiconductor Structures.* To be published in *Surface Science.*

Henini, M., M. L. Leadbeater, E. S. Alves, L. Eaves and O. H. Hughes (1989). *J. Phys.: Condens. Matter* 1, 3025.

Leadbeater, M. L., E. S. Alves, L. Eaves, M. Henini, O. H. Hughes, F. W. Sheard and G. A. Toombs (1988). *Semicond. Sci. Technol.* 3, 1060.

Leadbeater, M. L., E. S. Alves, L. Eaves, M. Henini, O. H. Hughes, A. Celeste, J. C. Portal, G. Hill and M. A. Pate (1989). *Phys. Rev. B* 39, 3438.

Leadbeater, M. L. and L. Eaves (1989). To be published.

Luryi, S. (1985). *Appl. Phys. Lett.* 47, 490.

Payling, C. A., E. S. Alves, L. Eaves, T. J. Foster, M. Henini, O. H. Hughes, P. E. Simmonds, F. W. Sheard and G. A. Toombs (1988). *Surf. Science* 196, 404.

Payne, M. C. (1986). *J. Phys. C: Solid State Phys.* 19, 1145.

Ricco, B. and M. Ya Azbel (1984). *Phys. Rev. B* 29, 1970.

Sheard, F. W. and G. A. Toombs (1988). *Appl. Phys. Lett.* 52, 1228.

Sheard, F. W. and G. A. Toombs (1989). *These Proceedings.*

Snell, B. R., K. S. Chan, F. W. Sheard, L. Eaves, G. A. Toombs, D. K. Maude, J. C. Portal, S. J. Bass, P. Claxton, G. Hill and M. A. Pate (1987). *Phys. Rev. Lett.* 59, 2806.

Tsuchiya, M., T. Matsusue and H. Sakaki (1987). *Phys. Rev. Lett.* 59, 2356.

Weil, T. and Vinter, B. (1987). *Appl. Phys. Lett.* 50, 1281.

Young, J. F., B. M. Wood, G. C. Aers, R. L. S. Devine, H. C. Liu, D. Landheer, M. Buchanan, A. L. Springthorpe and P. Mandeville (1988). *Phys. Rev. Lett.* 60, 2085.

Zaslavsky, A., V. J. Goldman and D. C. Tsui (1989). *Appl. Phys. Lett.* 53, 1408.